

Dynamical tidal response of neutron stars via scattering amplitudes

M.V.S. Saketh,^{1,*} Suprovo Ghosh,^{2,†} and Nils Andersson^{2,‡}

¹*International Centre for Theoretical Sciences, Tata Institute of Fundamental Research, Bangalore 560089, India*

²*Mathematical Sciences and STAG Research Centre,
University of Southampton, Southampton, United Kingdom.*

A key challenge of gravitational-wave astrophysics is distinguishing the nature of compact objects involved in binary coalescences, particularly whether they are black holes or neutron stars. Material bodies, like neutron stars, are distinguished from black holes by their tidal response, with both static and dynamical aspects (linked to the time-dependence of the tidal field) directly linked to the nature of the matter involved. The contrast with black holes, which are known to have a vanishing static tidal response, is clear. Measurements of the tidal response through gravitational observations constrains the neutron-star equation of state and provides insight into the physics of high-density matter. However, defining the tidal response of neutron stars in general relativity is challenging due to coordinate ambiguities and the complexity of connecting the star's response to binary dynamics and the associated gravitational waveforms. In this paper, we show how the dynamical tidal response of a neutron star can be systematically defined within the worldline effective field theory (EFT) framework, connecting the problem to gravitational-wave scattering off an isolated neutron star. These scattering amplitudes are computed both within the EFT, using standard quantum field-theory techniques, and within stellar perturbation theory (the corresponding ultraviolet theory), where the coupled metric and matter perturbation equations are solved in the stellar interior within general relativity and matched to the analytical Mano–Suzuki–Takasugi (MST) solutions in the exterior. We show how the scattering amplitude can be matched between effective theory and the ultraviolet theory to obtain the (frequency-dependent) dynamical tidal response. The results are found to be consistent with all known expectations, such as the static limit and the behaviour near the neutron star's resonant modes, while also recovering the imaginary part of the dominant oscillation mode induced by gravitational-wave dissipation. We conclude with a discussion of potential future improvements within both the EFT and the perturbation theory.

I. INTRODUCTION

Tidal dynamics induced in compact binary systems involving neutron stars provide opportunities to probe the nature of matter under extreme conditions. Although demonstrated already in the celebrated case of the first observed neutron-star-binary gravitational-wave signal GW170817 [1–3], the full potential of the strategy is expected to require the development of a new generation of instruments (Cosmic Explorer [4] in the USA and the Einstein Telescope [5] in Europe) in the next decade.

The tidal signature becomes prominent during the late stages of binary inspiral. It has two main contributions. The *static tide*, represented by the so-called Love numbers [6] and the associated tidal deformability (the quantity that is inferred from gravitational-wave data), was already constrained by the GW170817 data [7]. However, the static tide only relies on bulk properties, like the star's mass and radius. In contrast, the *dynamical tide*—commonly represented by resonances associated with the star's oscillation modes [8], linking the problem to asteroseismology—is sensitive to the specifics of the interior physics. The main dynamical tide contribution—associated with the star's fundamental oscillation mode, already included in state-of-the-art

waveform models [9, 10] used in the analysis of signals—only weakly so, but the presence (or absence) of lower frequency resonances depends directly on the composition and state of matter. The potential detectability of such features is a high-profile question with immediate relevance for nuclear physics [11–14].

Given the direct link to fundamental physics, there is an ongoing drive to model tidal dynamics to the precision required to meet the demands of future observations. This endeavor requires the development of fully relativistic models. However, efforts in this direction have long been hampered by technical issues. A key challenge is to define the tidal response in a manner that is amenable to quantifying the influence on binary dynamics and the associated gravitational-wave signal. This is rendered difficult due to the nonlinearities and coordinate freedom of general relativity. While there has been important progress in recent years in defining the dynamical tidal response of a neutron star [15–18], it remains unclear exactly how existing post-Newtonian (PN) Hamiltonians should be systematically augmented to incorporate the tidal response. This issue motivates the development of effective field theory (EFT) models [19–21]. The last two decades have witnessed the rise of EFTs applied to the two-body problem in general relativity, including the incorporation of spin [22–25], and other finite-size effects [26, 27] in a systematic PN expansion. The success of these approaches relies on the fact that various theoretical advances developed by particle physicists for computing Feynman diagrams/amplitudes in quantum field

* venkata.saketh@icts.res.in

† S.Ghosh@soton.ac.uk

‡ N.A.Andersson@southampton.ac.uk

theory can now (with some modifications) be applied to the binary problem. This has also spawned a host of other approaches (post-Minkowskian, heavy-particle effective theory, etc.) [28–30] involving the application of QFT techniques to gravitational-wave astrophysics.

The aim of this paper is to provide a robust definition and formulation of the dynamical tidal response within the worldline effective field theory (WEFT) framework, where a compact object is represented as a point particle moving along a worldline, supplemented by additional worldline degrees of freedom that encode finite-size effects such as tides. In this context, we contribute to recent demonstrations [15, 18] that the frequency-dependent tidal response can be obtained by matching solutions near the stellar surface. We improve upon previous approaches by establishing a direct connection to WEFT while avoiding complications associated with gauge freedom through a mapping between the tidal response and the gravitational Raman/Compton¹ scattering amplitude; the process of gravitational waves scattering off a relativistic compact object. We obtain the latter in relativistic stellar perturbation theory which is the ultraviolet (UV) theory², using analytical Mano-Sasaki-Takasugi (MST) solutions in the stellar exterior, and numerical solutions in the stellar interior. The tidal response follows by matching the two solutions. This construction neatly avoids issues of gauge invariance by providing a direct correspondence between observables.

The method has already been successfully applied to obtain the tidal response of black holes in a low-frequency expansion. Specifically, the static Love number [32], dissipation numbers at leading and next-to-leading order in frequency [33], and the running of the dynamical Love numbers [34], have been determined. There has also been work involving scalar perturbations [31]. A systematic description of the approach can be found in Ref. [35].

For neutron stars, the gravitational Raman scattering amplitude has been used to determine the static Love number and leading dissipation number by working consistently in a low-frequency expansion [36]. Here we extend existing WEFT results to approximately capture the full frequency dependence of the tidal response³. We then match with the arbitrary-frequency result for the scattering amplitude obtained in perturbation theory to get an analytical expression for the dynamical/frequency-dependent tidal response. We provide evidence that the

resulting expression for the dynamical tidal response offers a more realistic description of dynamical tides by studying the static limit and the behaviour near various stellar oscillation frequencies. Our work, therefore, brings us closer to a robust understanding of their influence on the orbital evolution of binary-neutron-star systems.

The paper is organized as follows: In Sec. II, we briefly review stellar perturbation theory in the interior and exterior of the star. The interior contains coupled metric and matter perturbation equations that will be solved numerically, while the exterior contains only metric perturbations treated analytically using the Mano-Sasaki-Takasugi formalism. Combining these solutions yields the tidal scattering phase for gravitational waves. In Sec. III, we introduce the worldline effective field theory description of a compact object coupled to gravity and compute the corresponding gravitational Raman scattering amplitude. In Sec. IV, we match the scattering amplitude in EFT and the scattering phase in perturbation theory to obtain an expression for the dynamical tidal response. We then proceed to present results obtained from this tidal response and compare them with previous results from the literature. We show where the new formalism improves upon previous results. Finally, Sec. V concludes with a discussion and possible future improvements.

We work with units $G = c = \hbar = 1$, and every instance of M should be treated as GM/c^2 , with dimensions of length.

II. STELLAR PERTURBATION THEORY: A BRIEF OVERVIEW

A. Perturbation equations in the interior.

We consider linear perturbations of a nonrotating, spherically symmetric relativistic star. The metric tensor describes the equilibrium background follows from

$$ds^2 = -e^{\nu(r)} dt^2 + e^{\lambda(r)} dr^2 + r^2(d\theta^2 + \sin^2\theta d\phi^2), \quad (1)$$

together with a perfect fluid stress-energy tensor

$$T^{\mu\nu} = (\varepsilon + p)u^\mu u^\nu + pg^{\mu\nu}, \quad (2)$$

where ε and p represent the energy and the pressure, respectively.

We introduce linear Eulerian perturbations ($h_{\mu\nu} = g_{\mu\nu} - g_{\mu\nu}^{(0)}$) to the metric, along with Lagrangian fluid displacement vector ξ^μ , perturbations of the fluid 4-velocity (u^μ), and thermodynamical quantities p and ε . Because of spherical symmetry, all perturbations can be decomposed into tensor spherical harmonics with angular indices (ℓ, m) . Adopting the Regge-Wheeler gauge and focusing on polar sector, the metric perturbations take

¹ We will refer to this as Raman scattering going forward, following the precedent set by Ref. [31].

² Stellar perturbation theory describes physics at high-frequencies and small length scales. Thus, we refer to it as the UV theory in this work.

³ It is important to mention Ref. [37], which obtained an approximate expression for the dynamical tidal response of a neutron star by combining worldline EFT and stellar perturbation theory. They found resonant behaviour corresponding to normal-mode oscillations, but faced some issues involving divergent intermediate terms and scheme-dependence when matching the EFT with the UV theory.

the form

$$h_{\mu\nu}^{\text{polar}} = -Y_{\ell m}(\theta, \phi) e^{-i\omega t} \times \begin{pmatrix} e^\nu r^\ell H_0(r) & i\omega r^{\ell+1} H_1(r) & 0 & 0 \\ i\omega r^{\ell+1} H_1(r) & e^\lambda r^\ell H_2(r) & 0 & 0 \\ 0 & 0 & r^{\ell+2} K(r) & 0 \\ 0 & 0 & 0 & r^{\ell+2} \sin^2 \theta K(r) \end{pmatrix}. \quad (3)$$

Meanwhile, using the gauge-freedom with the Lagrangian formulation, we set $u^\mu \xi_\mu = 0$, and expand the non-trivial components as

$$\begin{aligned} \xi^r(r) &= e^{-\lambda/2} r^{\ell-1} W(r) Y_{\ell m} e^{-i\omega t}, \\ \xi^\theta &= -r^{\ell-2} V(r) \partial_\theta Y_{\ell m} e^{-i\omega t}, \\ \xi^\phi &= -\frac{r^{\ell-2}}{\sin^2 \theta} V(r) \partial_\phi Y_{\ell m} e^{-i\omega t}. \end{aligned} \quad (4)$$

In summary, a general perturbation is described by the spacetime variables $H_0(r), H_1(r), H_2(r), K(r)$, alongside the fluid variables $W(r), V(r)$. These perturbation functions are, however, not all independent. We follow the formalism developed by Detweiler and Lindblom [38] to reduce the perturbation equations for the interior of the star to a system of four first-order differential equations for $H_1(r), K(r), W(r), X(r)$ (see Eq. 8-11 in Detweiler and Lindblom [38]), where $X(r)$ is an auxiliary variable proportional to the Lagrangian pressure perturbation, defined as

$$\begin{aligned} X(r) &= \omega^3 (p + \rho) e^{-\nu/2} V - r^{-1} p' e^{(\nu-\lambda)/2} W \\ &\quad + \frac{1}{2} (p + \rho) e^{\nu/2} H_0. \end{aligned} \quad (5)$$

The four independent perturbation equations are solved subject to boundary conditions. At the center of the star, $r = 0$, the solutions must be regular. The appropriate solutions are determined via the Taylor series expansion method described in Section II of Detweiler and Lindblom [38]. Outside the stellar surface, where the fluid perturbations vanish, we only have to solve for perturbations of the spacetime. In essence, the internal perturbations are matched to the standard Regge-Wheeler variable outside the star, as described in Sec. II B.

To close the fluid perturbation problem inside the star, we need to provide a matter equation of state; and a relation between perturbed (Lagrangian) pressure (ΔP) and energy density ($\Delta \varepsilon$). This is generally expressed in terms of the sound speed of the dense matter

$$\Delta P = \left(\frac{\partial P}{\partial \varepsilon} \right)_{n_i, T} \Delta \varepsilon = c_{ad}^2 \Delta \varepsilon, \quad (6)$$

where n_i are the densities of the constituent particles and T is the temperature of the star. Since we are interested

in the inspiral phase of a compact binary system, the temperature of the star is expected to be $\ll 1$ MeV [8, 39], and can be neglected for all practical purposes. Now, the exact expression for the sound speed for dense matter depends on the underlying thermodynamical conditions, the state and composition of dense matter. In this work, we are interested in $npe\mu$ matter, which maintains the background chemical equilibrium via the Urca reactions. At low temperatures, the reaction rates are slow enough (compared to the perturbation timescales) to maintain β -equilibrium [40]. Hence, the matter composition is practically frozen. In this scenario, the sound speed is given Eq. (6), which is very different from the equilibrium sound speed $c_{eq}^2 = \left(\frac{dP}{d\varepsilon} \right)$. If the reactions were to be fast enough (compared to the perturbation timescales), the perturbed pressure would maintain the same relationship as the equilibrium background, i.e.

$$\Delta P = c_{eq}^2 \Delta \varepsilon. \quad (7)$$

For a realistic neutron star model, the two sound speeds can be very different, and the difference $c_{ad}^2 - c_{eq}^2$ then gives rise to g -modes [41]. Given that the typical frequencies of low-order g -modes are $\sim 100 - 500$ Hz [42, 43], depending on the mass and interior composition of the neutron star, they can be resonantly excited by the tidal driving during the late stages of binary inspiral. At the low frequencies relevant for g -modes, the standard perturbation formulation meets with numerical difficulties [44]. To alleviate this, we adopt the strategy described in Appendix B of Kruger et al [44] (essentially using V instead of X as an independent variable).

B. Perturbation equations in the exterior

In the stellar exterior, the metric perturbation equations can be mapped to a single second-order differential equation, the Regge-Wheeler (RW) equation [45]. For a given mode, (i.e., ℓ, m, ω) the RW equation is

$$\frac{d^2 \phi}{dr_*^2} + [\omega^2 - V(r)] \phi = 0, \quad (8)$$

with

$$V(r) = f(r) \left[\frac{3f(r)}{r^2} + \frac{(\ell^2 + \ell - 3)}{r^2} \right], \quad (9)$$

where

$$r_* = r + 2M \log \left(\frac{r}{2M} - 1 \right) \quad (10)$$

is the tortoise coordinate and $f(r) = 1 - (2M/r)$.

Typically, one maps axial metric perturbations to the RW equation, while the polar perturbations considered here are mapped to the Zerilli equation. However, as the two sets of vacuum perturbations can be mapped to one another, we have chosen to work with the RW equation (which has a slightly simpler potential).

The RW scalar is related to the metric perturbations in the polar sector through the relations

$$\phi(r) = \frac{2M(1+n)f(r)(3M+nr)}{M(1+n)-r^3\omega^2}H_0(r) + \frac{r(n(1+n)r-3M(n+n^2+r^2\omega^2))}{M(1+n)-r^3\omega^2}K(r), \quad (11)$$

$$\begin{aligned} \frac{d\phi(r)}{dr} &= \frac{(1+n)(6M^2-n(1+n)r^2)}{r^4\omega^2-M(1+n)}H_0(r) + \frac{3Mr(-1-n+r^2\omega^2)}{r^4\omega^2-M(1+n)}H_0(r) \\ &+ \frac{nr(-3M+r(1+n))(1+n-r^2\omega^2)}{2Mf(r)(M(1+n)-r^3\omega^2)}K(r) + \frac{(3M-(n+1)r)(2n(1+n)+3r^2\omega^2)}{2f(r)(M(1+n)-r^3\omega^2)}K(r), \end{aligned} \quad (12)$$

where $n = (l-1)(l+2)/2$.

Moreover, the RW equation has analytical Mano-Sasaki-Takasugi (MST) solutions [46], given by sums over hypergeometric functions. A detailed discussion of the MST solutions for the RW equation can be found in Refs. [47]. Here, we only need some of the results from that paper.

As a second-order differential equation, the RW equation has two independent solutions, whose coefficients are determined by the boundary conditions at stellar surface. A convenient basis of solutions is given by

$$\begin{aligned} X_0^\nu &= (1-x)^{\nu+1+i\bar{\omega}} e^{i\bar{\omega}x} (-x)^{-i\bar{\omega}} \sum_{n=-\infty}^{n=\infty} \frac{\Gamma(-n-\nu+s-i\bar{\omega})\Gamma(2n+2\nu+1)}{\Gamma(n+\nu+1-s-i\bar{\omega})} a_n (1-x)^n \\ &\times {}_2F_1(-n-\nu+s-i\bar{\omega}, -n-\nu-s-i\bar{\omega}, -2n-2\nu; \bar{r}^{-1}), \end{aligned} \quad (13)$$

$$X_0^{-\nu-1} = X_0^\nu|_{\nu=-\nu-1}. \quad (14)$$

Here, a_n are coefficients which satisfy a recursion relation, and ν is called the renormalized angular momentum and is equal to ℓ in the limit $\omega \rightarrow 0$. Other variables are scaled in such a way that $\bar{\omega} = 2M\omega$, $\bar{r} = r/(2M)$ and $x = 1 - \bar{r}$. s is the spin weight of external perturbations, i.e., -2 for gravitational perturbations.

Used in Eq. (14), these expansions converge and are well-defined in the external region $r \in (2M, \infty)$. However, for a given frequency ω , their convergence radius is limited from above by $r \simeq \omega^{-1}$. Thus, the general RW scalar is given by

$$\phi = B_\nu X_0^\nu + B_{-\nu-1} X_0^{-\nu-1}. \quad (15)$$

The frequency-dependent ratio $B_{-\nu-1}/B_\nu$ encodes the rich internal physics of a neutron star. It is equal to 1 for black holes. For a neutron star, the relevant value is obtained by matching with metric perturbations at the stellar surface using Eq. (11) and Eq. (12) at $r = R$. This determines the solution in the stellar exterior.

C. Gravitational Raman scattering phase

To compute the scattering phase, we need to study the behaviour of $\phi(r)$ in the wave zone, i.e. in the limit $r \gg \omega^{-1}$. However, as mentioned earlier, the expansions in (14) do not converge in the regime $\omega r \gg 1$. In order to circumvent this issue, we note that the solutions themselves remain valid, and can be related to another

basis of solutions which have well-defined expansions in the far-zone.

The new solutions, denoted $X_C^{\nu/-\nu-1}$, are related to $X_0^{\nu/-\nu-1}$ according to

$$X_0^\nu = K_\nu X_C^\nu, \quad X_0^{-\nu-1} = K_{-\nu-1} X_C^{-\nu-1}, \quad (16)$$

where the expression for K_ν can be found in Eq. (3.32) of Ref. [47].⁴ The expansions for X_C^ν can also be found in Eq. (3.26) of Ref. [47].

Thus, in the wave-zone, we can instead work with

$$\phi(r) = B_\nu K_\nu X_C^\nu + B_{-\nu-1} K_{-\nu-1} X_C^{-\nu-1}. \quad (17)$$

In the limit $\omega r \gg 1$, this takes the form

$$\phi_{\ell\omega}(r)|_{r \rightarrow \infty} = A_{\ell\omega}^{\text{out}} e^{i\omega r} + A_{\ell\omega}^{\text{in}} e^{-i\omega r}, \quad (18)$$

with

$$\frac{A_{\ell\omega}^{\text{out}}}{A_{\ell\omega}^{\text{in}}} = (-1)^{\ell+1} e^{2i\delta_{\ell\omega}^{\text{NS}}} = \frac{e^{2i\bar{\omega} \log \bar{\omega}} A_-^\nu (1 + ie^{i\pi\nu} \mathcal{K}_{\text{NS}})}{A_+^\nu \left(1 - ie^{-i\pi\nu} \frac{\sin[\pi(\nu+i\bar{\omega})]}{\sin[\pi(\nu-i\bar{\omega})]} \mathcal{K}_{\text{NS}} \right)}, \quad (19)$$

and

$$\mathcal{K}_{\text{NS}} = \frac{B_{-\nu-1} K_{-\nu-1}}{B_\nu K_\nu}. \quad (20)$$

⁴ There is a small typo in Eq. (3.32) of Ref. [47]. In the numerator, it should be $(2\bar{\omega})^{s-\nu-r-1}$, and not $(2\bar{\omega})^{s-\nu-r}$.

The expressions for $A_{-/+}^\nu$ can be found in Eqs. (3.19) and (3.41) in Ref. [47]. In principle, we now have the scattering phase $\delta_{\ell\omega}$ as a function of the stellar boundary conditions. While this would be a satisfactory point to conclude the discussion of the perturbation theory as-

pects, it is convenient to instead (see later) define the so-called “tidal” phase

$$\delta_{\ell\omega}^{\text{tid}} = \delta_{\ell\omega}^{\text{NS}} - \Re\delta_{\ell\omega}^{\text{BH}}. \quad (21)$$

We can obtain $\Re\delta_{\ell\omega}^{\text{BH}}$ simply from Eq. (19) since we know that $B_{-\nu-1} = B_\nu$ for a black hole.

The advantage of this definition is that it removes contributions to the scattering phase that are common to both neutron stars and black holes, namely the non-tidal effects associated with propagation through the Schwarzschild spacetime exterior. This is useful for two reasons. First, from a practical point of view, state-of-the-art gravitational waveform models commonly use the black hole result as a baseline to which additional features, like neutron star tides, are added. Second, from a formal perspective; since black holes have vanishing static Love numbers and a tidal response that is suppressed relative to that of neutron stars, the resulting phase shift $\delta_{\ell\omega}^{\text{tidal}}$ is dominated by the neutron-star tidal response. We will make this statement more precise within the EFT framework in Sec. III. An additional benefit is that this definition eliminates the factors appearing in Eq. (19), namely $e^{2i\bar{\omega}\log\bar{\omega}}A_-^\nu/A_+^\nu$. These encode far-zone physics that is insensitive to the internal structure of the compact object [32]. Indeed, they are identical for black holes and neutron stars, as they do not depend on $B_{\nu(-\nu-1)}$.

Explicitly, we can write

$$2i\delta_{\ell\omega}^{\text{tidal}} = \log \left[\frac{(-1)^{\ell+1} e^{2i\bar{\omega}\log(\bar{\omega})} A_-^\nu (1 + ie^{i\pi\nu} \mathcal{K}_{\text{NS}})}{A_+^\nu \left(1 - ie^{-i\pi\nu} \frac{\sin[\pi(\nu+i\bar{\omega})]}{\sin[\pi(\nu-i\bar{\omega})]} \mathcal{K}_{\text{NS}} \right)} \right] - i\Im \log \left[\frac{(-1)^{\ell+1} e^{2i\bar{\omega}\log(\bar{\omega})} A_*^{-\nu} (1 + ie^{i\pi\nu} \mathcal{K}_{\text{BH}})}{A_+^\nu \left(1 - ie^{-i\pi\nu} \frac{\sin[\pi(\nu+i\bar{\omega})]}{\sin[\pi(\nu-i\bar{\omega})]} \mathcal{K}_{\text{BH}} \right)} \right], \quad (22)$$

where $\mathcal{K}_{\text{BH}} = K_{-\nu-1}/K_\nu$. Now, we can rewrite $(-1)^{\ell+1} e^{2i\bar{\omega}\log\bar{\omega}} (A_-^\nu/A_+^\nu) = e^{2i\delta_{\text{far}}}$, where δ_{far} is purely real and independent of the nature of the compact object. These factors therefore cancel, leaving

$$2i\delta_{\ell\omega}^{\text{tidal}} = \log \left(\frac{1 + ie^{i\pi\nu} \mathcal{K}_{\text{NS}}}{1 - ie^{-i\pi\nu} \frac{\sin[\pi(\nu+i\bar{\omega})]}{\sin[\pi(\nu-i\bar{\omega})]} \mathcal{K}_{\text{NS}}} \right) - i\Im \log \left(\frac{1 + ie^{i\pi\nu} \mathcal{K}_{\text{BH}}}{1 - ie^{-i\pi\nu} \frac{\sin[\pi(\nu+i\bar{\omega})]}{\sin[\pi(\nu-i\bar{\omega})]} \mathcal{K}_{\text{BH}}} \right), \quad (23)$$

Finally, we justify the terminology “tidal phase.” In the regime $M\omega \ll 1$, the dynamical tidal response of a black hole is negligible compared to that of a neutron star. Moreover, the static Love number of a black hole vanishes, while taking the real part of δ_{BH} removes dissipative effects associated with horizon absorption. Consequently, $\delta_{\ell\omega}^{\text{tidal}}$ may be viewed as the neutron-star phase shift with the universal point-particle contribution removed.

While this concludes the scattering problem in stellar perturbation theory, Eq. (23) is of limited utility for the binary problem unless we provide the means to extract the tidal response from it. To do this, we need to derive $\delta_{\ell m}^{\text{tidal}}$ as a function of the tidal response, after suitably defining the latter. With this in mind, we turn to describing a worldline EFT for a tidally deformed neutron star. The aim is to define a tidal response and relate it to the tidal scattering phase.

III. WORLDLINE EFFECTIVE FIELD THEORY INCLUDING DYNAMICAL TIDAL EFFECTS

We aim to model the compact object (an neutron star) as a point-particle following a worldline $z^\mu(\tau)$, adding degrees of freedom to capture the main finite-size effects. Formally, such a description is possible when the wavelength of the perturbations is much larger than the size of the compact object, i.e., when $R\omega \ll 1$, $M\omega \ll 1$. Within the worldline effective field theory framework, the sepa-

ration of scales naturally motivates an expansion in the perturbing frequency. In many applications, one assumes that the perturbing frequency ω is small compared to all intrinsic frequency scales of the system. For neutron stars with dynamical tides, however, this assumption generally breaks down. In particular, near resonance the perturbing frequency becomes comparable to the frequency $\omega_{f,g,\dots}$ of stellar oscillation modes, i.e., $\omega \sim \omega_{f,g,\dots}$. Moreover, a stratified neutron star supports a formally infinite spectrum of low-frequency gravity modes, implying that its tidal response cannot, in general, be captured by an expansion in $\omega/\omega_{f,g,\dots}$. We therefore adopt the weaker assumptions $M\omega \ll 1$ and $R\omega \ll 1$, while allowing ω to be comparable to the characteristic mode frequencies. This provides a framework capable of describing dynamical tidal effects, including resonant mode excitations.

Let us, first of all, write down a worldline action for a spinless particle with a quadrupolar degree of freedom,

coupled to external tidal fields as⁵

$$S = \int d\tau \left[-M + \frac{1}{2} Q^{\mu\nu}(\tau) E_{\mu\nu}(z^\mu(\tau)) \right] + S_Q \quad (24)$$

$$+ \frac{1}{16\pi} \int d^4x R\sqrt{-g} + S_{\text{GF}},$$

$$S = \int d\tau \left[-M - v^{[\mu} Q^{\nu][\rho} v^{\sigma]} R_{\mu\nu\rho\sigma} \right] + S_Q \quad (25)$$

$$+ \frac{1}{16\pi} \int d^4x R\sqrt{-g} + S_{\text{GF}},$$

where $d\tau = dt \sqrt{g_{\mu\nu}(dz^\mu/dt)(dz^\nu/dt)}$. The electric tidal field is $E_{\mu\nu}(x) = C_{\mu\alpha\nu\beta} v^\alpha v^\beta$, with $v^\alpha = dz^\alpha/d\tau$. The proper time τ is measured by a comoving, inertial observer sufficiently far away from the compact object, the mass of which is M . We use t to parametrize the worldline, and it is convenient to choose it to be identical to the proper time of the object when unperturbed (i.e., in

flat spacetime). $Q^{\mu\nu}(\tau)$ is used to model tidal deformation, which should ideally be represented by observable quantities. One way to achieve this is to write down an Ansatz for the quadrupole moment, expressing it as a linear functional of the tidal field $E_{\mu\nu}(z^\mu(\tau))$ [34]. The tidal response function can then be defined in terms of this linear functional, and may be regarded as the Green's function used to relate the source (the tidal field) to the excitation (the quadrupole moment). An equivalent approach would be to define the tidal response function in terms of the Feynman propagator of the quadrupole moment, which is more convenient as it enables the use of Feynman-diagram machinery for computing the Raman scattering amplitude. This follows since the Feynman propagator is related to a Green's function used for computing a field in the presence of a source, and is thus suitable for defining the tidal response. We should also impose the constraints $Q^{\mu\nu}v_\nu = 0$, $Q^\mu{}_\mu = 0$, as a physical quadrupole moment must have only 5 spacelike degrees of freedom. We will impose this when defining the tidal response further below.

The action in Eq. (25) determines the dynamics of the gravitational field in the environment of the compact object. Treating the problem perturbatively, it is convenient to expand the action in terms of deviations from flat spacetime, i.e., $g_{\mu\nu} = \eta_{\mu\nu} + h_{\mu\nu}$. In addition, we work in harmonic gauge where $\partial_\mu h^{\mu\nu} = (1/2)\partial^\nu h$. Since the object's motion may deviate due to external gravitational perturbations, we also expand the worldline as $z^\mu = u^\mu t + \delta z^\mu$ ($\delta z^\mu u^\nu \eta_{\mu\nu} = 0$, $\eta_{\mu\nu} u^\mu u^\nu = 1$, $\delta z^\mu \sim \mathcal{O}(h)$), where u^μ is the constant 4-velocity of the unperturbed object. We obtain

$$S = - \int dt \sqrt{1 + h_{\mu\nu} u^\mu u^\nu + 2h_{\mu\nu} u^\mu \dot{\delta z}^\nu + \delta z^\alpha u^\mu u^\nu \partial_\alpha h_{\mu\nu} + \eta_{\mu\nu} \dot{\delta z}^\mu \dot{\delta z}^\nu} M + S_Q - \int dt u^{[\mu} Q^{\nu][\rho} u^{\sigma]} \partial_\rho \partial_\nu h_{\mu\sigma} \quad (26)$$

$$+ \frac{1}{32\pi} \int d^4x \frac{1}{2} \partial_\lambda h_{\mu\nu} P^{\mu\nu,\rho\sigma} \partial^\lambda h_{\rho\sigma} + \mathcal{O}(h^3),$$

$$S \approx - \int M dt \sqrt{1 + \frac{\tilde{h}_{\mu\nu}}{m_{\text{pl}}} u^\mu u^\nu} - M \int dt \left(\delta z^\alpha f_\alpha + \frac{1}{2} \eta_{\mu\nu} \dot{\delta z}^\mu \dot{\delta z}^\nu \right) + S_Q - \frac{1}{m_{\text{pl}}} \int dt u^{[\mu} Q^{\nu][\rho} u^{\sigma]} \partial_\rho \partial_\nu \tilde{h}_{\mu\sigma} \quad (27)$$

$$+ \int d^4x \frac{1}{2} \partial_\lambda \tilde{h}_{\mu\nu} P^{\mu\nu,\rho\sigma} \partial^\lambda \tilde{h}_{\rho\sigma} + \mathcal{O}(h^3), \quad f_\alpha = \left(\frac{1}{2} u^\mu u^\nu \partial_\alpha \frac{\tilde{h}_{\mu\nu}}{m_{\text{pl}}} - u^\alpha \partial_\alpha \frac{\tilde{h}_{\mu\nu} u^\mu}{m_{\text{pl}}} \right)$$

$$\Rightarrow - \int M dt \left(\sqrt{1 + \frac{\tilde{h}_{\mu\nu}}{m_{\text{pl}}} u^\mu u^\nu} + \frac{1}{2} f^\nu \frac{1}{\partial_t^2} f_\nu \right) + S_Q - \frac{1}{m_{\text{pl}}} \int dt u^{[\mu} Q^{\nu][\rho} u^{\sigma]} \partial_\rho \partial_\nu \tilde{h}_{\mu\sigma} \quad (28)$$

$$+ \int d^4x \frac{1}{2} \partial_\lambda \tilde{h}_{\mu\nu} P^{\mu\nu,\rho\sigma} \partial^\lambda \tilde{h}_{\rho\sigma} + \mathcal{O}(h^3),$$

$$P^{\mu\nu,\rho\sigma} = \frac{1}{2} (\eta^{\mu\rho} \eta^{\nu\sigma} + \eta^{\mu\sigma} \eta^{\nu\rho} - \eta^{\mu\nu} \eta^{\rho\sigma}), \quad m_{\text{pl}}^{-1} \tilde{h}_{\mu\nu} = h_{\mu\nu}, \quad m_{\text{pl}}^2 = \frac{1}{32\pi}, \quad (29)$$

where in the third line, we have substituted the equation of motion for δz^μ at leading order in metric perturbation so as to eliminate it. This leaves behind a non-local recoil term ($-2^{-1} M \int dt f^\nu \partial_t^{-2} f_\nu$), accounting for the backreaction of the compact object in response to gravitational waves, and is essential to preserve gauge invariance [35]. Note that f^μ vanishes in the traceless-transverse gauge where $h^{\mu\nu} u_\nu = 0$.

⁵ We use the metric signature is $+, -, -, -$ in Sec. III for convenience, following the conventions in other works on scattering amplitudes. Note, however, that we ultimately compute a gauge-

invariant quantity to match with perturbation theory which has no dependence on the metric signature.

We do not perturb S_Q because perturbations in it can be typically absorbed into modifications of the mass and/or spin of the star [33]. Also, since we are only interested in matching with linear perturbation theory, we do not expand the 4-velocity that is contracted with the quadrupole tensor, and instead replace it with the background value u^μ .

The multi-graviton interactions, owing to the nonlinear nature of general relativity are encoded in $\mathcal{O}(h^3)$ terms which we have not explicitly written, but will be relevant in the analysis that follows. Note that we still write the action covariantly, without specializing to $u^\mu \equiv (1, 0, 0, 0)$. This is just a matter of convenience. However, we will label external graviton states based on their momentum and frequency in the frame defined by u^μ .

We now want to study the scattering amplitude of gravitational waves in the WEFT framework. Making use of standard quantum field theory techniques, we can write down the Feynman rules in momentum space some of which are shown in Fig. 1 where $\mathcal{P}^{\mu\nu} = \eta^{\mu\nu} - u^\mu u^\nu$. There are additional rules for multi-graviton interaction vertices which

$$\begin{aligned}
 & \text{Diagram 1: } \begin{array}{c} | \\ \cdots \\ M \end{array} = i \frac{M}{2m_{pl}} u^\mu u^\nu & \frac{(\mu, \nu) \quad q^\mu \quad (\rho, \sigma)}{q^2 + i\epsilon} = \frac{i}{q^2 + i\epsilon} P_{\mu\nu\rho\sigma} \\
 & \text{Diagram 2: } \begin{array}{c} q^\mu \\ \diagdown \\ \cdots \\ Q \end{array} = \frac{i}{m_{pl}} u^{[\mu} Q^{\nu][\rho} u^{\sigma]} q_\rho q_\nu & \xrightarrow{(q^\mu, h)_{\text{in}}} = \epsilon_{\mu\nu}^h(q) \\
 & \text{Diagram 3: } \begin{array}{c} \omega \\ \xrightarrow{Q^{\mu\nu}} \end{array} \quad \begin{array}{c} \xrightarrow{Q^{\rho\sigma}} \end{array} = iR^5 F(\omega) \frac{1}{2} (\mathcal{P}^{\mu\rho} \mathcal{P}^{\nu\sigma} + \mathcal{P}^{\mu\sigma} \mathcal{P}^{\nu\rho} - \frac{2}{3} \mathcal{P}^{\mu\nu} \mathcal{P}^{\rho\sigma}) & \xrightarrow{(q^\mu, h)_{\text{out}}} = \bar{\epsilon}_{\mu\nu}^h(q)
 \end{aligned}$$

FIG. 1: Some of the Feynman rules for WEFT in momentum space.

we ignore for the moment. There is also the contribution of the recoil term, whose contribution to the scattering amplitude vanishes at tree-level in a suitable gauge (for e.g., traceless-transverse gauge). Note also that the frequency in the rest frame of the compact object is conserved at each graviton-worldline vertex, owing to the integral over dt , but momentum is not conserved explicitly since we are treating the worldline as a heavy source against which gravitons are scattered. Note however that it is accounted for by the recoil term in the action in Eq. (28).

The tidal response function, which describes the dynamics of the induced quadrupole is given by $F(\omega)$, and enters the scattering problem via the propagator for the quadrupole moment as shown in Fig. 1. It is assumed to be invariant under $\omega \rightarrow -\omega$ and purely real. Note that it appears alongside the tensor

$$\mathcal{P}^{\mu\nu, \rho\sigma} = \frac{1}{2} (\mathcal{P}^{\mu\rho} \mathcal{P}^{\nu\sigma} + \mathcal{P}^{\mu\sigma} \mathcal{P}^{\nu\rho} - \frac{2}{3} \mathcal{P}^{\mu\nu} \mathcal{P}^{\rho\sigma}), \quad (30)$$

This ensures that the $\langle QQ \rangle$ propagator is symmetric, traceless and orthogonal to 4-velocity u^μ , ensuring that the dynamics of tidal quadrupole moment preserve the constraints $Q^{\mu\nu} u_\nu = 0$, $Q^\mu{}_\mu = 0$, at leading order in the metric perturbation. This way of defining the tidal response is completely equivalent to an explicit ansatz relating the frequency modes of tidal fields $E^{\mu\nu}$ and $Q^{\mu\nu}$ [34, 48, 49].

We can now immediately write down the leading order contribution to the Raman scattering process due to tidal

effects, shown in Fig. 2, as

$$\begin{aligned}
 i\mathcal{M}_{\omega; \vec{k}, h \rightarrow \vec{l}, h'} \Big|_{\text{tree level}} &= -\frac{1}{m_{pl}^2} u^\mu u^\sigma k_{[\mu} \epsilon_{\nu]}^{h'}(k) k_{\sigma]} \\
 &\times iR^5 F(\omega) \mathcal{P}^{\nu\rho, \beta\gamma} \times u^\alpha u^\delta l_{[\alpha} \bar{\epsilon}_{\beta]}^h(l) l_{\delta]}, \quad (31) \\
 &= \frac{-iR(R\omega)^4 F(\omega)}{16m_{pl}^2} \epsilon_{ij}^h(\vec{k}) \bar{\epsilon}_{h'}^{ij}(\vec{l}), \quad \omega = k \cdot u, \quad l \cdot u,
 \end{aligned}$$

where in the second equation we have chosen the polarization tensors in the traceless-transverse gauge, i.e., $\epsilon^{0\mu} = 0$, $\epsilon^\mu{}_\mu = 0$. We have also defined $\omega = k^0 = l^0$. Note that the covariant notation makes gauge invariance of the amplitude manifest in the first line in Eq. (31), since it is invariant under $\epsilon_h^{\mu\nu}(k) \rightarrow \epsilon_h^{\mu\nu}(k) + 2\zeta^{(\mu} k^{\nu)}$ (and similarly for $\epsilon_h^{\mu\nu}(l)$) thereby satisfying the gravitational Ward identity (or equivalently invariance under linearized diffeomorphisms/ coordinate transformations).

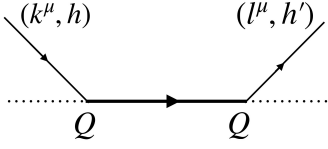


FIG. 2: Tree level, tidal contribution to Raman scattering

However, this is far from the only, or even the most relevant diagram for the scattering processes. For instance, there are several diagrams, such as those shown in Fig. 3, which do not encode any tidal effects. We will shortly show how to systematically include or discard them as needed.

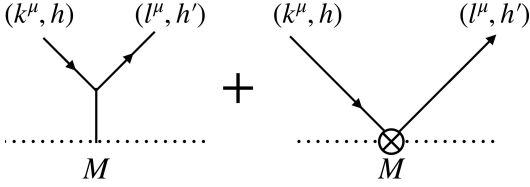


FIG. 3: Tree level, non-tidal contributions to Raman scattering. The \otimes vertex is due to the recoil term in Eq. (28), and vanishes in traceless transverse gauge. However, more generally, it is essential to preserve gauge invariance.

However, let us first understand the manner in which the contribution from Fig. 2 (or other such EFT diagrams) can be matched with the scattering phase in Eq. (19). To facilitate this comparison, we need to switch to a partial-wave basis. The Feynman diagrams naturally provide matrix elements of the S-matrix between fixed momentum and helicity states, i.e.,

$$i\langle \vec{l}', h' | T | \vec{k}, h \rangle = i\mathcal{M}(\omega; \vec{k}, h \rightarrow \vec{l}', h') 2\pi\delta(|\vec{k}| - |\vec{l}'|). \quad (32)$$

This can be converted to the ℓ, m, h basis using the relations [34]

$$|\vec{k}, h\rangle = \sum_{\ell=2}^{\infty} \sum_{m=-\ell}^{\ell} 2\pi \sqrt{\frac{2\ell+1}{2\pi|\vec{k}|}} D_{mh}^{\ell}(\hat{k}, 0) |\omega = |\vec{k}|, \ell, m, h\rangle, \\ \epsilon_{ij}^{h=\pm 2} = \sum_{m=-2}^{m=2} D_{mh}^{\ell=2} \langle i, j | \ell = 2, m \rangle, \quad (33)$$

where $\langle i, j | \ell = 2, m \rangle$ are the expansion coefficients of the usual spherical harmonics in the symmetric tracefree (STF) tensor basis. Thus, we have

$$i\langle \omega' \ell m h' | T | \omega \ell m h \rangle = i\mathcal{M}_{\omega, \ell; h \rightarrow h'} 2\pi\delta(\omega - \omega'), \quad (34)$$

where

$$i\mathcal{M}_{\omega, \ell; h \rightarrow h'} = \frac{-i(R\omega)^5 F(\omega)}{160m_{pl}^2\pi}, \quad (35)$$

at tree-level. Note that the above result does not depend on helicity. Finally, we can express the result in the parity basis, which is the diagonal partial-wave basis, using the relations

$$|\omega \ell m P\rangle = \frac{|\omega \ell m h = +2\rangle \pm (-1)^{\ell} |\omega \ell m h = -2\rangle}{\sqrt{2}}. \quad (36)$$

In the parity basis, we then have

$$i\langle \omega' \ell m P = + | T | \omega \ell m P = + \rangle = i\mathcal{M}_{P\omega\ell} 2\pi\delta(\omega - \omega'), \\ i\mathcal{M}_{P\omega\ell} = \frac{-i(R\omega)^5 F(\omega)}{80m_{pl}^2\pi}, \quad (37)$$

at tree-level. Finally, we use the operator relation, $S = I + iT$, to define the scattering phase in EFT as

$$2\pi\delta(\omega - \omega') e^{2i\delta_{\ell\omega}^{\text{EFT}}} = i\langle \omega' \ell m P = + | S | \omega \ell m, P = + \rangle \\ = 2\pi\delta(\omega - \omega') + i\langle \omega' \ell m P = + | T | \omega \ell m P = + \rangle. \quad (38)$$

Noting that we restrict ourselves to positive parities, this can be rewritten as

$$e^{2i\delta_{P=+, \omega}^{\ell m}} = 1 + i\mathcal{M}(\omega, \ell, P). \quad (39)$$

It is also convenient to define a new operator Δ , as shown in Ref. [35].

$$e^{2i\Delta} = S = I + iT, \\ 2\pi\delta(\omega - \omega') \delta_{\ell\omega}^{\text{EFT}} = \langle \omega' \ell m | \Delta | \omega \ell m \rangle. \quad (40)$$

In order for the EFT to be a faithful description of the stellar response, we expect δ^{EFT} to be identical to the phase obtained from perturbation theory in Eq. (19).

This concludes the discussion of how the amplitudes can be related to the scattering phase. However, there is a major inefficiency associated with the calculation of the right-hand side of equation Eq. (40). As mentioned before, T does not just receive contributions from diagrams containing tidal effects, i.e., the quadrupole moment. It also involves diagrams representing the process of waves scattering off the Schwarzschild background of the unperturbed star, e.g., the process in Fig. 3. This greatly increases our effort. In fact, one has to compute very high-loop diagrams corresponding to non-tidal (also referred to as far-zone) scattering processes in order to successfully use Eq. (40) to fix the tidal Love number [32, 34]. Efforts to compute high-loop, far-zone diagrams are still underway [31, 35, 50, 51].

For nonspinning neutron stars, this issue can be avoided by replacing Δ_{NS} with a different Hermitian operator that (i) isolates the dynamical tidal response of the star and (ii) possesses matrix elements that can be directly related to the tidal phase shift $\delta_{\ell\omega}^{\text{tidal}}$ appearing in Eq. (23). We will argue below that these requirements are fulfilled by defining

$$\tilde{\Delta}_{\text{tidal}}^{\text{NS}} = \Delta_{\text{NS}} - \Re\Delta_{\text{BH}}. \quad (41)$$

Then, by the relation of the scattering phase δ and the operator Δ in Eq. (40), the diagonal matrix elements of $\tilde{\Delta}_{\text{tidal}}^{\text{NS}}$ can be matched to $\delta_{\ell\omega}^{\text{tidal}}$ using Eq. (40). $\Re\Delta_{\text{BH}}$ should be understood as the corresponding operator for an EFT which has the same conservative dynamical tidal response as a black hole, but no dissipation (e.g., absorption associated with the event horizon).

However, it is still not clear how we plan to compute $\tilde{\Delta}_{\text{tidal}}^{\text{NS}}$ in the EFT without working out the high-order, far-zone, loop diagrams? Also, as we do not know the dynamical tidal response of a black hole, how do we use the matching to ultimately fix $F(\omega)$ which enters Δ_{NS} ? We will discuss these two questions in the following.

We start by defining (labeling) $\exp(\Re\Delta_{\text{BH}}) = 1 + iT_{\text{bh}}$, and $\exp\Delta_{\text{NS}} = 1 + iT_{\text{NS}}$, in accordance with Eq. (40). We can then write

$$\begin{aligned} e^{2i(\Delta_{\text{NS}} - \Re\Delta_{\text{BH}})} &= (1 + iT_{\text{NS}})(1 - iT_{\text{bh}}^\dagger) \\ &= 1 + i(T_{\text{NS}} - T_{\text{bh}}^\dagger) + T_{\text{NS}}T_{\text{bh}}^\dagger. \end{aligned} \quad (42)$$

At this point, we mathematically implement the approximation whereby we replace

$$\begin{aligned} T_{\text{NS}} &\rightarrow T_{\text{pp}} + T_{\text{tidal}}, \\ T_{\text{bh}} &\rightarrow T_{\text{pp}}, \end{aligned} \quad (43)$$

where T_{pp} is the non-trivial scattering operator for an EFT without tidal effects, i.e., no quadrupolar degree of freedom.

The idea is to approximate the black hole as a compact object with vanishing dynamical tidal response. Two further questions immediately arise: a) To what extent can a black hole's dynamical tidal response be ignored?, and b) Is this manner of implementing the approximation consistent? It is straightforward to answer the first question. From Eq. (37), it is clear that quadrupolar tidal effects first contribute at order $(M\omega)^5$ for black holes. However, owing to the vanishing static tidal response [52, 53], the leading quadrupolar tidal effects are dissipative and actually enter at order $(M\omega)^6$. Given that T_{bh} only encodes conservative contributions to the scattering process (since it is defined using $\Re(\Delta_{\text{BH}})$), it does not encode dissipation and thus tidal effects contribute only starting from $(M\omega)^7$. Comparing this to the leading order scaling for a neutron star in Eq. (40), it is clear that the dynamical tidal response of a black hole is suppressed by $(M/R)^5(M\omega)^2$, which is can be neglected (at least for our present purposes)⁶. One may object, suggesting that a different parameterization of the $\langle QQ \rangle$ propagator in Fig. 1 could have led to a prefactor of $(M\omega)^5$ in Eq. (37), in which case the suppression is just $(M\omega)^2$. This is true, but the parameterization in Fig. 1 was chosen in

accordance with known behaviour of the static tidal deformability of neutron stars, which approximately scales as the fifth power of compactness ($C = M/R$) [54, 55].

The second question, as to whether Eq. (43) is the mathematically correct way to implement the argument, is more subtle. The suggested replacement does not even hold approximately at all orders in $M\omega$. This is since T_{bh} is a finite and well-defined operator, whereas T_{pp} has divergences owing to far-zone, multi-loop diagrams starting at order $(M\omega)^7$ [34]. These divergences need to be regulated, and then cancelled by counter terms that are essentially tidal in nature, and thus the EFT of a point particle without tides is not meaningful at high orders in $(M\omega)$. To alleviate this issue, we can instead rewrite Eq. (43) using manifestly finite operators as

$$\begin{aligned} T_{\text{NS}} &\rightarrow \tilde{T}_{\text{pp}} + \tilde{T}_{\text{tidal}}, \\ T_{\text{bh}} &\rightarrow \tilde{T}_{\text{pp}}, \end{aligned} \quad (44)$$

where \tilde{T}_{pp} and \tilde{T}_{tidal} are obtained by subtracting the divergent pieces⁷ in T_{pp} and T_{tidal} via counter terms in the latter (possibly leaving behind some finite pieces scaling as $(M\omega)^7$ or higher with $\mathcal{O}(1)$ coefficients). In the first replacement, we can in fact choose these counter terms so that they cancel out in the sum (leaving behind logarithmic running dependence on the gravitational-wave frequency in the amplitudes), and the result is therefore exact. In the second replacement, however, since we do not know the dynamical tidal response of black holes, we are introducing errors of order $(M\omega)^7$ and higher, but unless the coefficients accompanying these terms are unexpectedly large, these errors can be expected to be small.

Now, using the fact that $1 + i\tilde{T}_{\text{pp}}$ is a unitary operator, we can then rewrite Eq. (42) as

$$e^{2i(\Delta_{\text{NS}} - \Re\Delta_{\text{BH}})} = e^{2i\Delta_{\text{tidal}}} = 1 + i\tilde{T}_{\text{tidal}} + \tilde{T}_{\text{tidal}}\tilde{T}_{\text{pp}}^\dagger. \quad (45)$$

Finally, it is convenient to expand the operators T_{BH}^\dagger in powers of M as

$$\tilde{T}_{\text{pp}} = MT_{(1)} + M^2T_{(2)} + \mathcal{O}(M^3), \quad (46)$$

$$\tilde{T}_{\text{tidal}} = T_{\text{tidal},(0)} + MT_{\text{tidal},(1)} + \mathcal{O}(M^2), \quad (47)$$

Substituting these expansions gives

$$\begin{aligned} e^{2i\Delta_{\text{tidal}}} &= 1 + iT_{\text{tidal},(0)} + M\left(iT_{\text{tidal},(1)} + T_{\text{tidal},(0)}T_{(1)}^\dagger\right) \\ &\quad + \mathcal{O}(M^2). \end{aligned} \quad (48)$$

Let us now evaluate the contributions at each order in M appearing on the right-hand side of Eq. (48). In this

⁶ In the PN framework, this represents an error at 3PN if we identify ω with approximately the orbital frequency, along with a suppression due to the large power of $M/R < 1$.

⁷ Divergences in T_{pp} are due to multi-loop diagrams starting at $(M\omega)^7$, whereas the divergences in T_{tidal} are due to counter terms included to cancel out the divergences in T_{pp} . There are also loop divergences in T_{tidal} which are discussed further below. They are not of concern here.

work, we restrict attention to the leading and next-to-leading terms, corresponding to orders M^0 and M^1 . In light of this restriction, the earlier discussion of far-zone divergences is not strictly necessary for the present analysis. Nevertheless, it lays the groundwork for extending the calculation to higher orders in future work.

The tree-level contribution to $T_{\text{tid},(0)}$ is simply the diagram in Fig 2. However, we can get other contributions that are independent of M by chaining together such diagrams as shown in Fig. 4. Summing over all diagrams

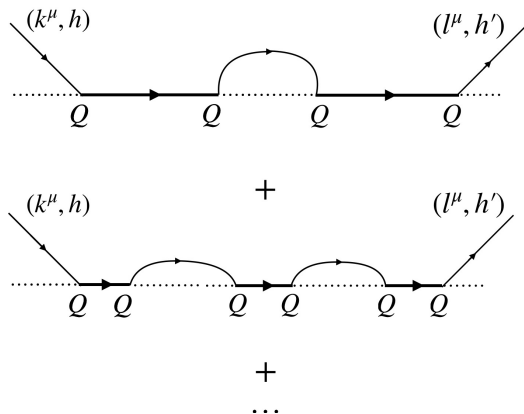


FIG. 4: Additional tidal contributions to the scattering process that do not involve mass insertions such as those in Fig. 5. These diagrams effectively resum the result of Fig. 2, and are required to account for backreaction due to gravitational radiation.

indicated in Fig. 4 yields the net tidal amplitude at M^0 . Referring to the contribution of Fig 2 as $T_{\text{tid},(0)}^{\text{tree}}$, we obtain⁸

$$T_{\text{tid},(0)} = \frac{T_{\text{tid},(0)}^{\text{tree}}}{1 - i \frac{T_{\text{tid},(0)}^{\text{tree}}}{2}}. \quad (49)$$

As a sanity check, we can use the unitarity of Δ_{tidal} at leading order in M to obtain the constraint $2\Im(T_{\text{tid},(0)}) = T_{\text{tid},(0)} T_{\text{tid},(0)}^\dagger$, from Eq. (48). It is easy to check that Eq. (49) satisfies this requirement, using the fact that $T_{\text{tid},(0)}^{\text{tree}}$ is Hermitian⁹.

⁸ The diagrams are formally divergent, but can be regulated in dimensional regularization to obtain the result presented in the text. In other schemes, they can lead to additional contributions which can be absorbed into a redefinition of $F(\omega)$ to once again obtain Eq. (49).

⁹ This follows from assuming that there is no viscosity, meaning $F(\omega)$ can only be imaginary at resonant poles. The latter is insufficient by itself if there is a continuum of resonant modes (i.e., gapless degrees of freedom), and thus we further assume that the spectrum is discrete in the relevant regime of ω in this work.

Moving on to linear order in M in the RHS of Eq. (48), the first contribution to $T_{\text{tid},(1)}$ is given in Fig. 5. This diagram requires the three-graviton vertex, but fortunately, it can be evaluated using the ingredients already available in Ref. [56].

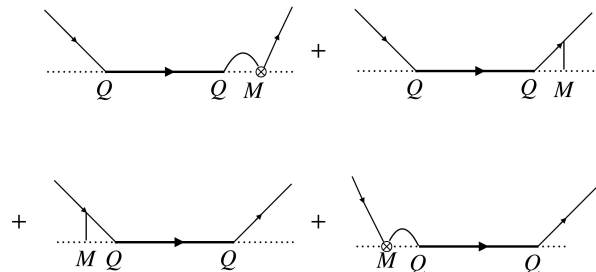


FIG. 5: The simplest diagrams at linear order in M . The loop leads to an infrared divergence as well, which does not show up in any observables. The labels for incident and outgoing momenta have been suppressed to avoid cluttering.

As before, this diagram can be chained together with multiple copies of the diagram in Fig. 2 to create many more contributions to $T_{\text{tid},(1)}$ such as those shown in Fig. 6.

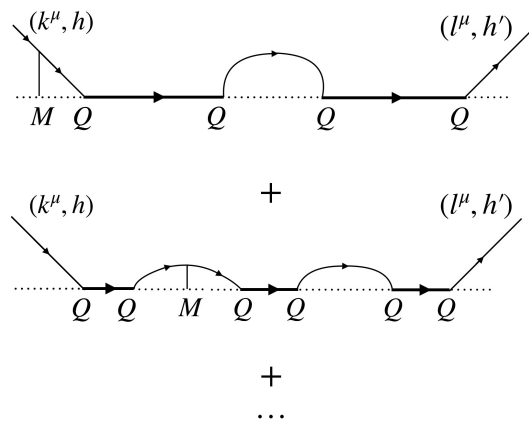


FIG. 6: Additional contributions to $T_{\text{tid},(1)}$ involving one mass insertion.

Strictly speaking, we should use the Feynman rule for the 3-graviton vertex to compute such chains to obtain a summed version. However, we leave a proper analysis of this for the future and instead “guess” a form that is consistent with the leading order piece and satisfies the unitarity constraints. The required result takes the form

$$T_{\text{tid},(1)} = \frac{\Im(T_{\text{tid},(1)}^{\text{simple}})}{1 - i \frac{T_{\text{tid},(0)}^{\text{tree}}}{2}} + \frac{\Re(T_{\text{tid},(1)}^{\text{simple}})}{\left(1 - i \frac{T_{\text{tid},(0)}^{\text{tree}}}{2}\right)^2} \quad (50)$$

where we refer to the contribution from Fig. 5 as¹⁰ $T_{\text{tid},(1)}^{\text{simple}}$. Now, defining

$$G_{(1)} = T_{\text{tid},(1)} - iT_{\text{tid},(0)}T_{(1)}^\dagger, \quad (51)$$

the unitarity of Δ_{tidal} at linear order in M yields

$$2\Im G_{(1)} = T_{\text{tid},(0)}G_{(1)}^\dagger + G_{(1)}T_{\text{tid},(0)}^\dagger. \quad (52)$$

This is satisfied by Eq. (50) provided $\Im(T_{\text{tid},(1)}^{\text{simple}}) = T_{\text{tid},(0)}^{\text{tree}}T_1$, which in turn follows trivially from taking the imaginary part of the sum of diagrams in Fig. 5 with the help of the cutting rules. We have also used $T_{(1)}^\dagger = T_{(1)}$ to obtain this relation, which follows simply from the fact that $T^{(1)}$ is the contribution due to the diagrams in Fig. 3, which have no propagators that can be cut.

Then, we can rewrite

$$G_{(1)} = T_{\text{tid},(1)} - iT_{\text{tid},(0)}T_{(1)}^\dagger = \frac{\Re(T_{\text{tid},(1)}^{\text{simple}})}{\left(1 - i\frac{T_{\text{tid},(0)}^{\text{tree}}}{2}\right)^2}. \quad (53)$$

Finally, defining a frequency operator $\hat{\omega}$ as $\hat{\omega}|\vec{k}, h\rangle = |\vec{k}||\vec{k}, h\rangle$, and using the results of Ref. [56], we can write the operator relation

$$\Re(T_{\text{tid},(1)}^{\text{simple}}) = T_{\text{tid},(0)}^{\text{tree}}2\pi\hat{\omega}. \quad (54)$$

The analysis can be extended straightforwardly (albeit with increasing tediousness) to higher orders in M . However, we restrict our attention to linear order in M in this work. Combining the results, we obtain

$$e^{2i\Delta_{\text{tidal}}} = 1 + i\frac{T_{\text{tid},(0)}^{\text{tree}}}{1 - i\frac{T_{\text{tid},(0)}^{\text{tree}}}{2}} \left(1 + \frac{2\pi M\hat{\omega}}{1 - i\frac{T_{\text{tid},(0)}^{\text{tree}}}{2}}\right) \quad (55)$$

which is unitary to $\mathcal{O}(M^2)$. This can be improved by simply resumming Eq. (55) by adding terms $\mathcal{O}(M^2)$ and higher as

$$e^{2i\Delta_{\text{tidal}}} = \frac{1 + i\frac{T_{\text{tid},(0)}^{\text{tree}}}{2}(1 + 2\pi M\hat{\omega})}{1 - i\frac{T_{\text{tid},(0)}^{\text{tree}}}{2}(1 + 2\pi M\hat{\omega})}, \quad (56)$$

which is unitary to all orders in M . Now, using

$$\delta_{\ell\omega}^{\text{EFT,tidal}} = \frac{\langle\omega, \ell, m, P|\Delta_{\text{tidal}}|\omega_1, \ell, m, P\rangle}{2\pi\delta(\omega - \omega_1)}, \quad (57)$$

and the result for the tree-level tidal phase in Eq. (37), we obtain the scattering phase as

$$e^{2i\delta_{\ell\omega}^{\text{EFT,tidal}}} = \frac{1 - i\frac{(R\omega)^5 F(\omega)}{160m_{\text{pl}}^2\pi}(1 + 2\pi M|\omega|)}{1 + i\frac{(R\omega)^5 F(\omega)}{160m_{\text{pl}}^2\pi}(1 + 2\pi M|\omega|)} \quad (58)$$

This is what we need to match with the scattering phase from perturbation theory, given earlier in Eq (23), in order to determine $F(\omega)$.

IV. RESULTS

After studying the Raman scattering process in the effective theory and how the problem connects to neutron-star perturbation theory, we arrived at two expressions for the tidal scattering phase; Eqs. (58) and (23). Matching these, we obtain the tidal response function as

$$F(\omega) = -\frac{160m_{\text{pl}}^2\pi}{(R\omega)^5(1 + 2\pi M|\omega|)} \tan \delta_{\ell\omega}^{\text{tidal}} \quad (59)$$

It is convenient to relate this result to the usual definition of the dimensionless tidal response as $k_2(\omega) = -(3/4)F(\omega)$. This leads to

$$\begin{aligned} k_2^{\text{EFT}}(\omega) &= \frac{120m_{\text{pl}}^2\pi}{(R\omega)^5(1 + 2\pi M|\omega|)} \tan \delta_{\ell\omega}^{\text{tidal}}, \\ &= \frac{15}{4(R\omega)^5(1 + 2\pi M|\omega|)} \tan \delta_{\ell\omega}^{\text{tidal}}, \end{aligned} \quad (60)$$

where $e^{2i\delta_{\ell\omega}^{\text{tidal}}}$ is obtained from the analytical MST solutions using Eq. (19).

We naturally want to explore the tidal response we have derived and compare with previous results. This is, however, problematic as no appropriately validated results in this direction exist. A rigorous assessment of the results would require computing the corresponding gravitational waveforms (or the corresponding phase evolution) to facilitate a direct comparison. Given that we would need to connect to the orbital evolution, this would require a fair amount of extra work which we leave for the future. It is also relevant to note there are currently no validated models that account for the presence of low-frequency g-modes in the tidal response. State-of-the-art waveform models [9, 10] only account for the dynamical tide of the fundamental neutron-star mode, which is not expected to pass through resonance before binary merger. Additionally, typical waveform models involve free parameters that are tuned to match numerical simulations. Hence, it is unclear if such a comparison would actually help distinguish between expressions for the tidal response. What we actually need is progress on alternatives to the problem, such as the relativistic mode-sum approach proposed in Ref. [17], and then to come up with observables that can be consistently compared across methods. Once completed, that approach would allow an apples-to-apples comparison, which would be very welcome.

As an approximate diagnostic, we may contrast our results with earlier expressions for the dynamical tidal response, such as those from Ref. [18]. Admittedly, this comparison assumes that the overall strategy to infer the tidal response through matching makes sense. Even this comparison is not entirely straightforward, since the tidal responses are defined somewhat differently. However, the comparison highlights the qualitative features, like particularly the behavior near resonances, and we

¹⁰ $T_{\text{tid},(1)}$ receives contributions from loop diagrams, and thus we cannot refer to the simplest diagram as a tree diagram.

can make meaningful statements regarding the improvements brought by the present analysis. As an example of this we can explore the low-frequency limit in which the response is characterized by a single static Love number, common to all approaches up to normalization conventions. A useful benchmark for any dynamical tide model is how accurately the low-frequency behavior reproduces the static limit. As we will demonstrate, our model performs very well in that respect.

A. Tidal response near quasinormal modes

We start by considering the dynamical tidal response $k_2(\omega)$ obtained from Eq. (60) near a few resonant modes for a specific neutron-star model. For this example, we focus on the BSk22 equation of state from the Brussels-Montreal collaboration [57–59]. This is a convenient choice because we can then make direct comparisons with the results from [18]. We will not provide results for other models here, because we only aim for a proof-of-principle at this stage.

Our first model is a neutron star with mass $M = 1.4 M_\odot$ and radius $R = 13.04$ km. A few of relevant quasinormal modes (QNMs) for this model are $g_c = 0.00643 \text{ km}^{-1}$, $g_1 = 0.00577 \text{ km}^{-1}$, $g_2 = 0.0039 \text{ km}^{-1}$, and $f = 0.0345 \text{ km}^{-1}$. In Fig. 7, we illustrate the tidal response near a couple of the g-modes. Meanwhile, Fig. 8 shows the tidal response near the f-mode.

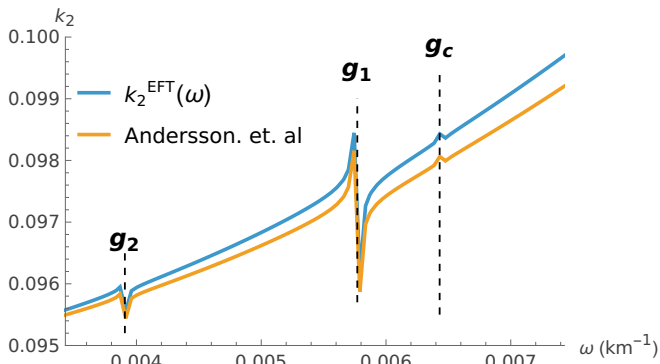


FIG. 7: Illustrating the dynamical tidal response near resonant frequencies; in this case the highest frequency g-modes for the chosen BSk model. The tidal response obtained from Eq. (60) is labeled “ $k_2^{\text{EFT}}(\omega)$ ”, while that used in Ref. [18] is labeled “Andersson. et. al”. Given that the two sets of results are very close, the considerably more advanced formalism we have brought appears to have only a modest effect on the final result near the g-modes.

It is evident that Eq. (60) is sensitive to resonant features and the results in Fig. 7 and 8 closely resemble the results from [18]. This is an important consistency check, since one of the primary applications of the dynamical tidal response is to capture the nontrivial dynamics that

arise when the orbital frequency enters resonance with a stellar eigenfrequency. As expected, we find that the strongest resonant behavior occurs near the f-mode, see Fig. 8. This demonstrates why the f-mode is the only mode currently incorporated into waveform models. Its dominance is evident in all dynamical tide calculations. Overall, these results indicate that the tidal response obtained from our new model differs only slightly from previous results in Ref. [18]. If anything, the results show that the analysis in [18] was already rather good (at least for less massive neutron stars).

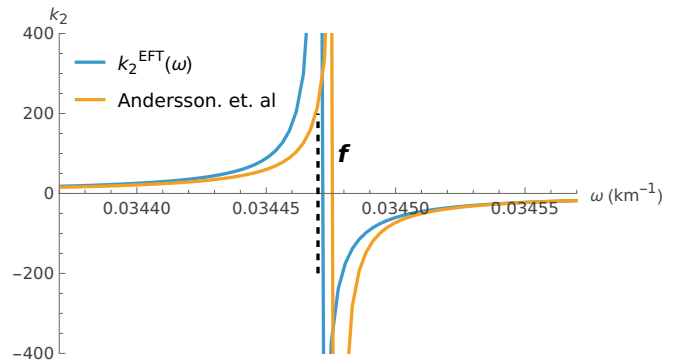


FIG. 8: A zoomed in plot providing a detailed comparison near the dominant f-mode. Both tidal responses roughly show resonant behaviour close to the QNM frequency. The new result seems to align slightly more closely with the f-mode, but this shift is quite negligible.

While the f-mode frequencies (the location of the tidal resonance) are very close, Fig. 8 suggests that the new model moves slightly closer to the known QNM value. This is more clearly visible as the stellar mass increases. This is shown in Fig. 9, where we plot the comparison between the tidal responses in the current work and the result from Ref. [18] near the f-mode for a star with mass $1.98 M_\odot$, and radius $R = 12.59$ km. The dashed vertical line shows the true value of the real part of the f-mode frequency. It is clear that the earlier result in Ref. [18] has a larger offset (of around 0.1%) towards higher frequencies, whereas $k_2^{\text{EFT}}(\omega)$ exhibits resonant behaviour very close to the expected point. This suggests an improved capturing of tidal resonances for more massive neutron stars.

B. The low-frequency behaviour

The low-frequency behaviour of the tidal response provides a crucial sanity check of any dynamical tide model. Given this, it makes sense to explore how our results approach the known results for the static Love number [6]. It was already demonstrated in [36] that the scattering problem can be matched consistently in the low-frequency limit to obtain the expected static tidal

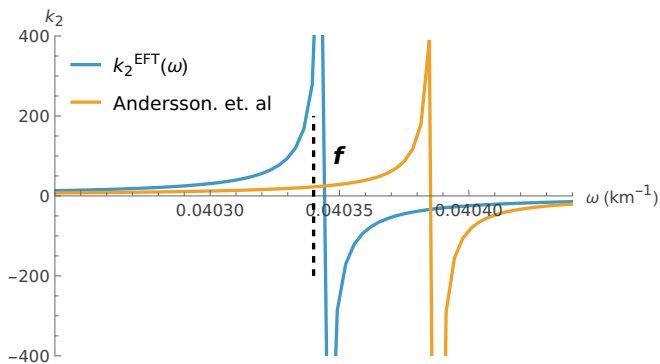


FIG. 9: A zoomed in plot providing a detailed comparison near the dominant f-mode for $M = 1.98M_{\odot}$, and $R = 12.59$ km. Note that $k_2(\omega)$ shows resonance behaviour very close to the expected f-mode frequency (indicated by the dashed, vertical red line) whereas the earlier result in Ref. [18] shows a slight offset towards higher frequencies.

response. Nevertheless, the comparison we want to make is not straightforward because the interior neutron-star problem is known to be tricky at low-frequencies. The problem is associated with terms in the solutions that scale with inverse powers of the frequency [15, 18, 36]. This makes it difficult to approach the limit numerically. Nevertheless, we can establish that the tidal response smoothly approaches the expected result. We can also make a direct comparison to other results in this regime, like those from [18].

In Fig. 10 we show the percent deviation from the static Love number for the tidal response obtained from Eq. (60) alongside that from Ref. [18]. This figure demonstrates the main improvement brought by our new model, which has significantly decreased the systematic deviation noted in [18].

C. Estimating the imaginary part of the f-mode

Another useful check of the relationship between the tidal scattering phase and the tidal response given in Eq. (58) may be performed by assuming that a single mode dominates the tidal response in the vicinity of resonance and inferring the imaginary part of the associated QNM frequency. In essence, the strategy extends the “near-zone boundary condition” proposal from Lindblom et al. [60]. They demonstrated how neutron-star QNM frequencies could be calculated by incorporating the outgoing-wave boundary condition weak-field near zone (essentially at the surface of the star). This led to an accurate calculation of the f-mode oscillation frequency, but the imaginary part (the damping rate) could only be obtained with $\sim 10\%$ accuracy [18].

Specifically, QNMs correspond to frequencies for which only outgoing radiation is present at infinity. Since the

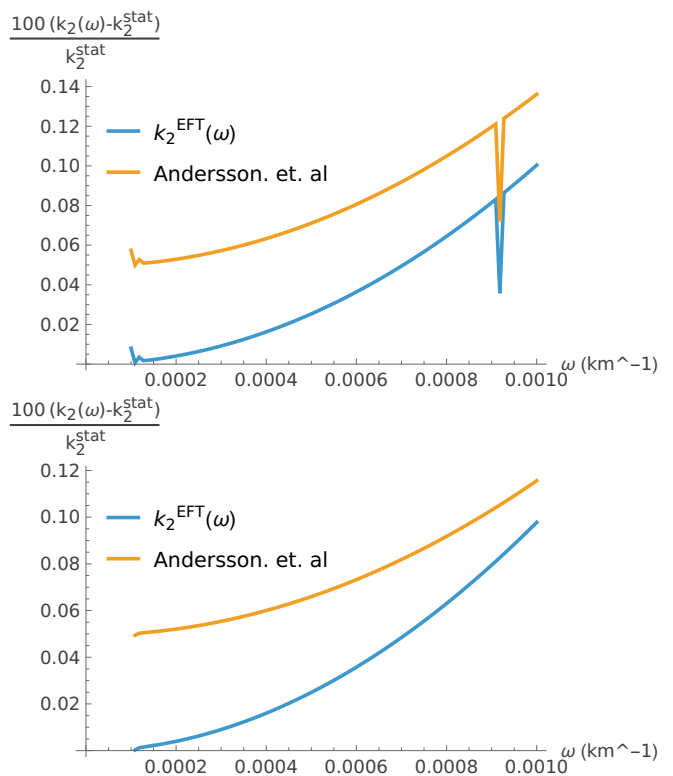


FIG. 10: Low-frequency behaviour of the tidal response for the BSk22 equation of state and two stellar models. The top panel shows results for a star with $M = 1.4M_{\odot}$ and $R = 13.04$ km while the bottom panel represents a model with $M = 1.98M_{\odot}$ and $R = 12.59$ km. The results show that the new model has significantly improved on the systematic error discussed in [18]. It is also worth noting the slight wiggles at the lowest frequencies in the top panel. These indicate the low-frequency region where numerically solving the neutron-star perturbation equations is difficult.

exponential of the scattering phase is closely related to the ratio of the coefficients of outgoing and incoming waves, as shown in Eq. (19), it is expected to diverge at each QNM frequency ($\omega = \omega_{\text{qnm}}$). Using the relation

$$\frac{A_{\ell\omega}^{\text{out}}}{A_{\ell\omega}^{\text{in}}} \approx (-1)^{\ell+1} e^{2i\delta_{\ell\omega}^{\text{pp}}} e^{2i\delta_{\ell\omega}^{\text{tidal}}}, \quad (61)$$

and noting that the point-particle contribution to the phase does not contain information about the stellar matter properties, the neutron-star QNMs are expected to be associated with divergences in $e^{2i\delta_{\ell\omega}^{\text{tidal}}}$. Making use of Eq. (58), this leads to the condition

$$\begin{aligned} 1 &= -i(R\omega_{\text{qnm}})^5 \frac{F(\omega_{\text{qnm}})}{160m_{\text{pl}}^2\pi} (1 + 2\pi M\omega_{\text{qnm}}) \\ &= i(R\omega_{\text{qnm}})^5 \frac{4k_2(\omega_{\text{qnm}})}{15} (1 + 2\pi M\omega_{\text{qnm}}). \end{aligned} \quad (62)$$

Since $k_2(\omega)$ is real, the above relation cannot be satisfied for real frequencies, indicating the need for a complex

solution, as expected given that the QNMs should be damped by gravitational-wave emission.

An approximate solution for the imaginary part of the dominant f-mode may be obtained by assuming that the f-mode dominates the tidal response in the near-resonance region. To do this, we make the ansatz

$$k_2(\omega) = \frac{A}{1 - (\omega/\omega_0)^2}, \quad (63)$$

where ω_0 and A can be extracted by fitting $k_2(\omega)$ close to the f-mode. As seen from Fig. 8, ω_0 is very close to the real part of the f-mode frequency. Substituting Eq. (63) into Eq. (62) and expanding around $\omega_{\text{qnm}} \approx \omega_0 + \delta\omega$, we

obtain

$$\delta\omega \approx -i \frac{2\omega_0}{15} A (R\omega_0)^5 (1 + 2\pi M\omega_0) + \mathcal{O}(A^2). \quad (64)$$

The leading-order correction to the mode frequency is negative and imaginary, as expected. Implementing this strategy, we have evaluated this expression for the BSk equation of state and for three stellar models, including the two previously considered. The results are compared with the known values of the imaginary part of the f-mode in Table. I. As discussed earlier, we identify ω_0 with the real part of the f-mode frequency and we already know from comparisons with Ref [18] in Figs. 7, 8, that this is accurately determined from our calculation.

M/M_\odot	R (km)	$\Re(\omega_f)$ (km $^{-1}$)	$-\Im(\omega_f)$ (km $^{-1}$)	A	ω_0	$-\Im(\delta\omega)$ (km $^{-1}$)	$100 \times \frac{i\Im(\omega_f) - \delta\omega}{i\Im(\omega_f)}$
1.4	13.04	0.03447	1.2646×10^{-5}	0.1036	0.03447	1.2646×10^{-5}	$\leq 0.002\%$
1.6	12.98	0.03628	1.58536×10^{-5}	0.09187	0.03628	1.58537×10^{-5}	$\leq 0.001\%$
1.98	12.59	0.04034	2.14998×10^{-5}	0.06781	0.4034	2.15×10^{-5}	$\leq 0.001\%$

TABLE I: Imaginary part of the f-mode for stellar models determined from the BSk22 equation of state as predicted by the pole in Eq. (58) using the numerically fitted analytical ansatz in Eq. (63). Note that the disagreement is essentially negligible and is thus a significant improvement over previous results in Ref. [18] using the method advanced in Ref. [60]

We find that the predicted imaginary parts of the calculated f-modes agree with the known values exceptionally well. In fact, they represent a dramatic improvement of the results reported in [18]. This shows the robustness and physical validity of our method.

It is relevant to add a couple of comments on the numerical results provided in table I. The calculation is subject to several sources of uncertainty, including the finite resolution and interpolation of the equation of state table, as well as the numerical accuracy of the solvers used for the stellar interior and perturbation equations. However, these effects are common to both determinations of the mode frequency, namely the direct output of the mode solver and the estimate obtained from Eq. (64), since they use the same interior solution for the background of the star as well as the numerical solutions for the metric and matter perturbations. Consequently, any systematic bias arising from these sources is expected to affect the two methods in a similar manner and should therefore have only a limited impact on the comparison.

D. Discussion of results

Before concluding, it is important to emphasize that the ultimate objective of any definition of relativistic tidal response is not merely to characterize the response itself, but to incorporate tidal effects into binary dynamics and, ultimately, into gravitational waveform models. Consequently, the merits of a given approach to dynamical tides should be assessed not only by the form of the resulting tidal response, but also by the theoretical and computational framework that underlies it.

A key advantage of the present formulation is that it is directly connected to the underlying dynamics of the compact object within the standard PN-EFT frameworks. The tidal response derived here provides a systematic prescription for incorporating tidal dynamics into the worldline action of Eq. (25), from which their influence on the motion of a compact object subject to an external field can be computed in a consistent manner. Following earlier works such as Ref. [61], it can also be incorporated straightforwardly into a binary Hamiltonian within the PN formalism. Moreover, our approach provides a systematic treatment of the exterior spacetime and yields a manifestly gauge-invariant definition of the tidal response.

While several previous works have formulated relativistic tidal response within a worldline EFT framework [26, 33, 34, 36, 48, 61, 62], they typically either restrict attention to the low-frequency adiabatic regime, thereby excluding resonant phenomena, or model the tidal quadrupole as a single harmonic oscillator associated with the f -mode. In contrast, our construction avoids both the adiabatic approximation and the one-mode assumption. Instead, it is rigorously matched to stellar perturbation theory in a gauge-invariant manner, enabling the full dynamical tidal response of the compact object to be captured within the EFT.

An equally important advance of the present framework, building on developments in Refs. [34, 35, 51], is its systematic improvability. The expression for the tidal response in Eq. (60) can be refined by computing additional diagrams at higher orders in M , thereby incorporating progressively more of the exterior spacetime dynamics. Indeed, several ingredients are already available and can be incorporated directly into the formalism, including some higher-order loop corrections [56] and resummed tail effects [50, 56]. Such flexibility is particularly valuable in the era of precision gravitational-wave astronomy, where efficient, systematic, and internally consistent treatments of the binary problem are essential for reducing waveform systematics and fully exploiting the capabilities of current and future detectors.

The fact that our approach correctly reproduces resonant behaviour (see Fig. 7, Fig. 8, and Fig. 9), possesses a consistent low-frequency limit without introducing systematic errors (see Fig. 10), and enables accurate determination of the imaginary parts of the f -mode frequencies (see Table. I) all lend support to the validity of the method. However, these phenomenological successes should be viewed as consequences of a broader achievement: the construction of a gauge-invariant, systematically improvable EFT framework for relativistic dynamical tides in neutron stars that is directly suited for applications to compact-binary dynamics and waveform modeling.

V. CONCLUSION AND FUTURE WORK

We have developed a new frequency-dependent model for the tidal response of a neutron star, as defined within the WEFT framework, matching to results from relativistic stellar perturbation theory, explicitly without a strict low-frequency expansion. Our proof-of-principle results show that the dynamical tidal response, including the regime near resonant frequencies, can be consistently determined up to corrections of order $(M\omega)^2$ relative to the leading contribution. Such corrections are generally negligible during binary inspiral, which is relevant at 3PN order w.r.t the leading order tidal effects. Furthermore, we have outlined a general procedure that can be systematically extended to incorporate higher-order corrections in $M\omega$ as additional EFT results (i.e., newly computed

diagrams) become available. Consequently, the framework is designed to naturally accommodate both current and future developments within WEFT.

Our model provides an analytical expression for the conservative dynamical tidal response of a neutron star, Eq. (60), which reduces to the well-known result for the static Love number in the appropriate low-frequency limit [6, 36]. Comparing our results to an earlier expression obtained in Ref. [18], we demonstrate that the two models lead to qualitatively similar behavior, including the expected features near resonant frequencies. However, the tidal response derived in this work is significantly more accurate for both low-frequencies (see Fig. 10) and near resonant mode frequencies (as evidenced by the accurate determination of the imaginary part of star’s fundamental mode in Table. I).

Although the numerical differences between the tidal response obtained in this work and those derived in previous work are generally relatively small, it is important to emphasize that the way in which our tidal response enters the binary dynamics is particularly transparent. Unlike most other approaches, which tend to define the tidal response through the ratio of growing and decaying metric perturbation modes in the region near the star’s surface or through other characteristics of the perturbed stellar metric, our definition is based solely on a quantity appearing in the worldline action in the EFT. This quantity directly encodes the dynamical properties of the neutron star and can be straightforwardly incorporated into the computation of the corresponding PN Hamiltonian, e.g. by following the analysis from for example Ref. [61]. Furthermore, by relating the tidal response to an observable quantity, namely the tidal scattering phase, we avoid ambiguities associated with coordinate freedom.

This work can be extended in several directions. On the EFT side, a straightforward extension would be to incorporate effects at order $(M\omega)^2$, which have already been partially calculated in other contexts [34, 56, 61, 63]. This is also the order at which the EFT tidal response requires renormalization due to loop divergences, leading to a logarithmic frequency dependence in related observables [34, 61]. Another important direction would be the inclusion of viscous fluid dissipation within the stellar interior, recently shown to have significant implications for the presence of exotic matter in neutron-star interiors. [39, 64]. Such effects were previously studied within a low-frequency approximation [36], but are expected to become more significant near resonances and should therefore be incorporated into the dynamical tidal response. Finally, one can instead focus on using the WEFT to derive a two-body Hamiltonian and compute gravitational waveforms, contributing to the development of models for binary-neutron-star and black-hole-neutron-star searches and parameter inference.

On the stellar perturbation side, one may explore a range of neutron-star equations of state, including exotic scenarios like dark-matter admixed models. Arguably, the most interesting technical development would be to

incorporate spin effects. This will require modifications to both the perturbation theory and EFT frameworks, but also brings new physics into play. In particular, we will be able to quantify the effect of rotational frame dragging and the impact of tidal resonances associated with inertial modes (which require the gravito-magnetic coupling). We plan to explore some of these directions in future work.

ACKNOWLEDGEMENTS

We thank Jan Steinhoff, and Zihan Zhou for valuable discussions. The research of M.V.S.S. is supported by the

National Post-Doctoral Fellowship (PDF/2025/004764), ANRF, Government of India. N.A. and S.G. gratefully acknowledge support from the STFC via Grant No. ST/Y00082X/1.

-
- [1] LIGO Scientific Collaboration and Virgo Collaboration. Properties of the binary neutron star merger gw170817. *Physical Review X*, 9(1), January 2019. Publisher Copyright: © 2019 authors. Published by the American Physical Society.
- [2] B. P. Abbott et al. Gw170817: Observation of gravitational waves from a binary neutron star inspiral. *Phys. Rev. Lett.*, 119:161101, Oct 2017.
- [3] M. Soares-Santos et al. The Electromagnetic Counterpart of the Binary Neutron Star Merger LIGO/Virgo GW170817. I. Discovery of the Optical Counterpart Using the Dark Energy Camera. *Astrophys. J. Lett.*, 848(2):L16, 2017.
- [4] David Reitze et al. Cosmic Explorer: The U.S. Contribution to Gravitational-Wave Astronomy beyond LIGO. *Bull. Am. Astron. Soc.*, 51(7):035, 2019.
- [5] Adrian Abac et al. The Science of the Einstein Telescope. *JCAP*, 03:081, 2026.
- [6] Tanja Hinderer. Tidal love numbers of neutron stars. *The Astrophysical Journal*, 677(2):1216–1220, April 2008.
- [7] B. P. Abbott et al. GW170817: Measurements of neutron star radii and equation of state. *Phys. Rev. Lett.*, 121(16):161101, 2018.
- [8] Dong Lai. Resonant oscillations and tidal heating in coalescing binary neutron stars. *Mon. Not. Roy. Astron. Soc.*, 270:611, 1994.
- [9] Tanja Hinderer, Andrea Taracchini, Francois Foucart, Alessandra Buonanno, Jan Steinhoff, Matthew D. Duez, Lawrence E. Kidder, Harald P. Pfeiffer, Mark A. Scheel, Béla Szilágyi, Kenta Hotokezaka, Koutarou Kyutoku, Masaru Shibata, and Cory W Carpenter. Effects of neutron-star dynamic tides on gravitational waveforms within the effective-one-body approach. *Physical review letters*, 116 18:181101, 2016.
- [10] Adrian Abac, Tim Dietrich, Alessandra Buonanno, Jan Steinhoff, and Maximiliano Ujevic. New and robust gravitational-waveform model for high-mass-ratio binary neutron star systems with dynamical tidal effects. *Phys. Rev. D*, 109:024062, Jan 2024.
- [11] Geraint Pratten, Patricia Schmidt, and Natalie Williams. Impact of dynamical tides on the reconstruction of the neutron star equation of state. *Phys. Rev. Lett.*, 129:081102, Aug 2022.
- [12] A.R. Counsell, F. Gittins, N. Andersson, and I. Tews. Interface modes in inspiralling neutron stars: A gravitational-wave probe of first-order phase transitions. *Physical Review Letters*, 135(8), August 2025.
- [13] Hang Yu and Nevin N. Weinberg. Dynamical tides in coalescing superfluid neutron star binaries with hyperon cores and their detectability with third-generation gravitational-wave detectors. *Monthly Notices of the Royal Astronomical Society*, 470(1):350–360, May 2017.
- [14] Fabian Gittins, Harsh Narola, Thibaut Wouters, Peter T. H. Pang, Tanja Hinderer, and Chris Van Den Broeck. Detecting Tidal Resonances in Binary Neutron Stars. 6 2026.
- [15] Abhishek Hegade K. R., Justin L. Ripley, and Nicolás Yunes. Dynamical tidal response of nonrotating relativistic stars. *Phys. Rev. D*, 109(10):104064, 2024.
- [16] Abhishek Hegade K. R., Yumu Yang, Mauricio Hippert, Jacquelyn Noronha-Hostler, Jorge Noronha, and Nicolás Yunes. Dynamical tidal response of neutron stars as a probe of dense-matter properties. 3 2026.
- [17] Abhishek Hegade K. R., K. J. Kwon, Tejaswi Venumadhav, Hang Yu, and Nicolas Yunes. The Good, the Bad, and the Subtle: Relativistic mode sums for neutron-star tidal response. 5 2026.
- [18] Nils Andersson, Rhys Counsell, Fabian Gittins, and Suprovo Ghosh. Tidal response of a relativistic star. *Phys. Rev. D*, 113(6):064051, 2026.
- [19] Michèle Levi. Effective Field Theories of Post-Newtonian Gravity: A comprehensive review. *Rept. Prog. Phys.*, 83(7):075901, 2020.
- [20] Rafael A. Porto. The effective field theorist’s approach to gravitational dynamics. *Phys. Rept.*, 633:1–104, 2016.
- [21] Walter D. Goldberger. Effective field theories of gravity and compact binary dynamics: A snowmass 2021 whitepaper. 2022.
- [22] Michele Levi and Jan Steinhoff. Spinning gravitating objects in the effective field theory in the post-Newtonian scheme. *JHEP*, 09:219, 2015.
- [23] Zhengwen Liu, Rafael A. Porto, and Zixin Yang. Spin Effects in the Effective Field Theory Approach to Post-Minkowskian Conservative Dynamics. *JHEP*, 06:012, 2021.
- [24] Gihyuk Cho, Rafael A. Porto, and Zixin Yang. Gravitational radiation from inspiralling compact objects: Spin

- effects to the fourth post-Newtonian order. *Phys. Rev. D*, 106(10):L101501, 2022.
- [25] Sylvain Marsat. Cubic order spin effects in the dynamics and gravitational wave energy flux of compact object binaries. *Class. Quant. Grav.*, 32(8):085008, 2015.
- [26] Walter D. Goldberger and Ira Z. Rothstein. An Effective field theory of gravity for extended objects. *Phys. Rev. D*, 73:104029, 2006.
- [27] Manoj Kumar Mandal, Pierpaolo Mastrolia, Hector O. Silva, Raj Patil, and Jan Steinhoff. Renormalizing love: tidal effects at the third post-newtonian order. *Journal of High Energy Physics*, 2024, 2023.
- [28] Thibault Damour. Gravitational scattering, post-minkowskian approximation, and effective-one-body theory. *Phys. Rev. D*, 94:104015, Nov 2016.
- [29] Gregor Kälin and Rafael A. Porto. Post-Minkowskian Effective Field Theory for Conservative Binary Dynamics. *JHEP*, 11:106, 2020.
- [30] Rafael Aoude, Kays Haddad, and Andreas Helset. On-shell heavy particle effective theories. *JHEP*, 05:051, 2020.
- [31] Mikhail M. Ivanov, Yue-Zhou Li, Julio Parra-Martinez, and Zihan Zhou. Gravitational Raman Scattering in Effective Field Theory: A Scalar Tidal Matching at $O(G^3)$. *Phys. Rev. Lett.*, 132(13):131401, 2024. [Erratum: *Phys.Rev.Lett.* 134, 159901 (2025)].
- [32] Mikhail M. Ivanov and Zihan Zhou. Vanishing of Black Hole Tidal Love Numbers from Scattering Amplitudes. *Phys. Rev. Lett.*, 130(9):091403, 2023.
- [33] M. V. S. Saketh, Jan Steinhoff, Justin Vines, and Alessandra Buonanno. Modeling horizon absorption in spinning binary black holes using effective worldline theory. *Phys. Rev. D*, 107(8):084006, 2023.
- [34] M. V. S. Saketh, Zihan Zhou, and Mikhail M. Ivanov. Dynamical tidal response of Kerr black holes from scattering amplitudes. *Phys. Rev. D*, 109(6):064058, 2024.
- [35] Mikhail M. Ivanov, Yue-Zhou Li, Julio Parra-Martinez, and Zihan Zhou. Gravitational Raman Scattering: a Systematic Toolkit for Tidal Effects in General Relativity. 2 2026.
- [36] M. V. S. Saketh, Zihan Zhou, Suprovo Ghosh, Jan Steinhoff, and Debarati Chatterjee. Investigating tidal heating in neutron stars via gravitational Raman scattering. *Phys. Rev. D*, 110:103001, 2024.
- [37] Sayan Chakrabarti, T erence Delsate, and Jan Steinhoff. New perspectives on neutron star and black hole spectroscopy and dynamic tides. 4 2013.
- [38] S. Detweiler and L. Lindblom. On the nonradial pulsations of general relativistic stellar models. *Astrophys. J.*, 292:12–15, May 1985.
- [39] Suprovo Ghosh, Bikram Keshari Pradhan, and Debarati Chatterjee. Tidal heating as a direct probe of strangeness inside neutron stars. *Phys. Rev. D*, 109(10):103036, 2024.
- [40] Raymond F. Sawyer. Bulk viscosity of hot neutron-star matter and the maximum rotation rates of neutron stars. *Phys. Rev. D*, 39:3804–3806, Jun 1989.
- [41] A. R. Counsell, F. Gittins, and N. Andersson. The impact of nuclear reactions on the neutron-star g-mode spectrum. *Mon. Not. Roy. Astron. Soc.*, 531(1):1721–1729, 2024.
- [42] Rhys Counsell, Fabian Gittins, Nils Andersson, and Pantelis Pnigouras. Neutron star g modes in the relativistic Cowling approximation. *Mon. Not. Roy. Astron. Soc.*, 536(2):1967–1979, 2024.
- [43] Vinh Tran, Suprovo Ghosh, Nicholas Lozano, Debarati Chatterjee, and Prashanth Jaikumar. g-mode oscillations in neutron stars with hyperons. *Phys. Rev. C*, 108(1):015803, 2023.
- [44] C.J. Kr uger, W.C.G. Ho, and N. Andersson. Seismology of adolescent neutron stars: Accounting for thermal effects and crust elasticity. *Physical Review D*, 92(6), 2015.
- [45] Tullio Regge and John A. Wheeler. Stability of a schwarzschild singularity. *Phys. Rev.*, 108:1063–1069, Nov 1957.
- [46] Shuhei Mano, Hisao Suzuki, and Eiichi Takasugi. Analytic solutions of the Regge-Wheeler equation and the postMinkowskian expansion. *Prog. Theor. Phys.*, 96:549–566, 1996.
- [47] Marc Casals and Adrian C. Ottewill. High-order tail in Schwarzschild spacetime. *Phys. Rev. D*, 92(12):124055, 2015.
- [48] Walter D. Goldberger and Ira Z. Rothstein. Dissipative effects in the worldline approach to black hole dynamics. *Phys. Rev. D*, 73:104030, 2006.
- [49] Walter D. Goldberger, Jingping Li, and Ira Z. Rothstein. Non-conservative effects on spinning black holes from world-line effective field theory. *JHEP*, 06:053, 2021.
- [50] Chih-Hao Chang, Chia-Hsien Shen, and Zihan Zhou. Gravitational Sommerfeld Effects: Formalism, Renormalization, and Perturbation to $O(G^{10})$. 4 2026.
- [51] Simon Caron-Huot, Miguel Correia, Giulia Isabella, and Mikhail Solon. Gravitational Wave Scattering via the Born Series: Scalar Tidal Matching to $O(G^7)$ and Beyond. *Phys. Rev. Lett.*, 135(19):191601, 2025.
- [52] Taylor Binnington and Eric Poisson. Relativistic theory of tidal love numbers. *Phys. Rev. D*, 80:084018, 2009.
- [53] Thibault Damour and Alessandro Nagar. Relativistic tidal properties of neutron stars. *Phys. Rev. D*, 80:084035, 2009.
- [54] Kent Yagi and Nicol as Yunes. Approximate universal relations for neutron stars and quark stars. *Phys. Rept.*, 681:1–72, 2017.
- [55] Andrea Maselli, Vitor Cardoso, Valeria Ferrari, Leonardo Gualtieri, and Paolo Pani. Equation-of-state-independent relations in neutron stars. *Phys. Rev. D*, 88:023007, 2013.
- [56] Walter D. Goldberger and Andreas Ross. Gravitational radiative corrections from effective field theory. *Phys. Rev. D*, 81:124015, 2010.
- [57] S. Goriely, N. Chamel, and J. M. Pearson. Hartree-Fock-Bogoliubov nuclear mass model with 0.50 MeV accuracy based on standard forms of Skyrme and pairing functionals. *Phys. Rev. C*, 88(6):061302, December 2013.
- [58] J M Pearson, N Chamel, A Y Potekhin, A F Fantina, C Ducoin, A K Dutta, and S Goriely. Unified equations of state for cold non-accreting neutron stars with brussels–montreal functionals – i. role of symmetry energy. *Monthly Notices of the Royal Astronomical Society*, 481(3):2994–3026, 12 2018.
- [59] N. N. Shchepochin, N. Chamel, and J. M. Pearson. Unified equations of state for cold nonaccreting neutron stars with brussels-montreal functionals. iv. role of the symmetry energy in pasta phases. *Phys. Rev. C*, 108:025805, Aug 2023.
- [60] Lee Lindblom, Gregory Mendell, and James R. Ipser. Relativistic stellar pulsations with near-zone boundary conditions. *Phys. Rev. D*, 56:2118–2126, Aug 1997.

- [61] Manoj K. Mandal, Pierpaolo Mastrolia, Hector O. Silva, Raj Patil, and Jan Steinhoff. Renormalizing Love: tidal effects at the third post-Newtonian order. *JHEP*, 02:188, 2024.
- [62] Jan Steinhoff, Tanja Hinderer, Alessandra Buonanno, and Andrea Taracchini. Dynamical Tides in General Relativity: Effective Action and Effective-One-Body Hamiltonian. *Phys. Rev. D*, 94(10):104028, 2016.
- [63] Gustav Uhre Jakobsen, Gustav Mogull, Jan Plefka, and Benjamin Sauer. Tidal effects and renormalization at fourth post-Minkowskian order. *Phys. Rev. D*, 109(4):L041504, 2024.
- [64] Suprovo Ghosh, José Luis Hernández, Bikram Keshari Pradhan, Cristina Manuel, Debarati Chatterjee, and Laura Tolos. Tidal heating in binary inspiral of strange quark stars. *Phys. Rev. D*, 112(8):084072, 2025.